

VU Research Portal

Simultaneous spark plasma synthesis and consolidation of WC/Co composites

Locci, A.M.; Orru, R.V.A.; Cao, G.

published in

Journal of Materials Research
2005

DOI (link to publisher)

[10.1557/JMR.2005.0096](https://doi.org/10.1557/JMR.2005.0096)

document version

Publisher's PDF, also known as Version of record

[Link to publication in VU Research Portal](#)

citation for published version (APA)

Locci, A. M., Orru, R. V. A., & Cao, G. (2005). Simultaneous spark plasma synthesis and consolidation of WC/Co composites. *Journal of Materials Research*, 20(3), 734-741. <https://doi.org/10.1557/JMR.2005.0096>

General rights

Copyright and moral rights for the publications made accessible in the public portal are retained by the authors and/or other copyright owners and it is a condition of accessing publications that users recognise and abide by the legal requirements associated with these rights.

- Users may download and print one copy of any publication from the public portal for the purpose of private study or research.
- You may not further distribute the material or use it for any profit-making activity or commercial gain
- You may freely distribute the URL identifying the publication in the public portal ?

Take down policy

If you believe that this document breaches copyright please contact us providing details, and we will remove access to the work immediately and investigate your claim.

E-mail address:

vuresearchportal.ub@vu.nl

Simultaneous spark plasma synthesis and consolidation of WC/Co composites

Antonio Mario Locci

Dipartimento di Ingegneria Chimica e Materiali, Centro Studi sulle Reazioni Autopropaganti (CESRA), and Unità di Ricerca del Consorzio Interuniversitario per la Scienza e Tecnologia dei Materiali (INSTM), Università degli Studi di Cagliari, 09123 Cagliari, Italy

Roberto Orrù^{a)} and Giacomo Cao^{b)}

Dipartimento di Ingegneria Chimica e Materiali, Centro Studi sulle Reazioni Autopropaganti (CESRA), and Unità di Ricerca del Consorzio Interuniversitario per la Scienza e Tecnologia dei Materiali (INSTM), Università degli Studi di Cagliari, 09123 Cagliari, Italy; and PROMEA Scarl, c/o Dipartimento di Fisica, Cittadella Universitaria di Monserrato, 09042 Monserrato (CA), Italy

(Received 29 July, 2004; accepted 15 December, 2004)

The single-step synthesis and densification of the WC–6Co cemented carbide starting from elemental powders was obtained by the spark plasma sintering (SPS) technique. The operating conditions that guarantee the complete conversion of the reactants to the desired full dense material have been identified. Specifically, under the application of 800 A and a mechanical pressure of 40 MPa for about 200 s, a product with relative density higher than 99%, hardness of 14.97 ± 0.35 GPa, and 12.5 ± 1.0 MPa m^{0.5} fracture toughness was obtained. A kinetic investigation of the SPS process was also performed. It revealed that an intermediate phase, i.e., W₂C, is the first carbide formed during the carburization process. It was observed that the synthesis and sintering stages take place simultaneously. It was also found that as the applied pulsed current intensity was augmented, the synthesis/sintering time required decreased significantly.

I. INTRODUCTION

It is well known that WC–Co cermet materials possess attractive mechanical properties, i.e., wear/abrasion resistance, high hardness, and elastic modulus, as well as a good fracture toughness, which make them extensively used in several areas, in particular, as cutting and machining tools.^{1–3} Therefore, due to their practical importance, several studies have been conducted in the last decades to investigate and improve their mechanical properties.

Typically, dense cemented tungsten carbides are produced following two steps. First, powders of WC are synthesized, and subsequently, the obtained powders are subjected to a sintering/consolidation process after they are mixed with the metal binder.

Several methods of synthesizing WC powders have been proposed. Carburization of tungsten powder at high temperature is typically used to produce tungsten carbide.^{4,5} With the goal of obtaining nanostructured

powders, other techniques including, for example, ball milling,^{6–8} spray conversion process (SCP),⁹ and spray thermal decomposition,⁵ have also been used recently. Moreover, 99% pure WC powders with 1–2 μm particle size were prepared from elements through the Self-propagating high-temperature synthesis (SHS) method in the presence of a highly exothermic mixture (Mg + Teflon) as reaction promoter.¹⁰

Regarding the consolidation stage, besides conventional sintering methods, hot pressing (HP) and hot isostatic pressing (HIP),^{5,8} as well as other more recently developed techniques—for example, spark plasma sintering (SPS)^{9,11,12}—are also used for the preparation of dense WC–Co composites. In particular, cemented functional gradient materials (FGM) carbide with four gradient layers (from 6 to 20 wt% Co) was fabricated by an automatic SPS system starting from fine (average particle size less than 0.5 μm) WC powders.¹²

The synthesis and consolidation by a single-step process starting from elemental powders was obtained by field-activated pressure assisted combustion synthesis (FAPACS)¹³ and high-frequency induction heated combustion synthesis (HFIHCS).¹⁴

Along these lines, in the present investigation, the simultaneous synthesis and densification of WC–6 wt%

Address all correspondence to these authors.

^{a)}e-mail: orru@visnu.dicm.unica.it

^{b)}e-mail: cao@visnu.dicm.unica.it

DOI: 10.1557/JMR.2005.0096

Co using the SPS apparatus was investigated when starting from commercial elemental reactants. This technique, which basically consists of the simultaneous application of a pulsed electric current and a mechanical load through the reacting sample, was demonstrated to be very attractive for the preparation of dense bodies including nanostructured materials.^{15–18}

Initial powder mixtures used in previous studies,^{9,11,12} which took advantage of the SPS technique for the obtainment of dense cemented carbides, consisted of previously synthesized tungsten carbide to be subjected to the sintering/consolidation stage. This is not the case of the proposed study. Moreover, the nominal composition of the cemented composites investigated by SPS in the cited studies, i.e., WC–10 wt% Co,⁹ WC–10Co–0.8VC,¹¹ and WC–Co FGM materials,¹² is different from the one considered in this work.

A kinetic investigation on the transformation process of initial elemental reactants to the desired composite is first performed in this work. Subsequently, the influence of the applied electric current on the synthesis process dynamics as well as product characteristics is examined. A comparison of the mechanical properties of the synthesized materials with the analogues available on the market, as well as those prepared using the other techniques mentioned above, is also reported.

II. EXPERIMENTAL MATERIALS AND METHODS

The characteristics of the starting powders used in the present investigation as well as their sources are reported in Table I. The tungsten and graphite powders were weighted in equiatomic ratio, and the cobalt powder was added in an amount sufficient to obtain a concentration of 6 wt% in the final product. All powders were dry mixed in a SPEX 8000 (Metachen, NJ) mill for 30 min. Milling was done in a stainless steel jar using alumina balls.

A SPS 515 apparatus produced by Sumitomo Coal Mining Co. Ltd. (Tokyo, Japan), was used to synthesize dense WC/Co. It combines a 50 kN uniaxial press with a direct current (dc) pulsed current generator (10 V, 1500 A, 300 Hz) to simultaneously provide a pulsed electric current through the sample and the graphite die containing it, together with a mechanical load through the die plungers. Two cylindrical graphite blocks (diameters of 80 mm and 30 mm, and height of 40 mm) were placed between the upper plunger and the upper electrode, as well as the

lower plunger and the lower electrode. The die, plungers, and blocks were all made of AT101 graphite (Atal s.r.l. Sull'adda, Italy).

About 11 g powder mixture was first cold-compacted inside the die (outside diameter, 30 mm; inside diameter, 15 mm; height, 30 mm). To protect the die and facilitate the sample release after synthesis, a 99.8% pure graphite foil (0.13 mm thick, Alfa Aesar, Karlsruhe, Germany) was inserted between the internal surface of the die and between the top and the bottom surface of the sample and the graphite plungers (14.7 mm diameter, 20 mm height). In addition, with the aim to minimize the heat loss by thermal radiation, the die was covered with a layer of graphite felt. The die was then placed inside the reaction chamber of the SPS apparatus and the system was evacuated (10 Pa). This step was followed by the application of 40 MPa mechanical pressure through the plungers. The experiment is initiated with the application of a previously set constant value of the electric current for a given time. Temperatures were measured during synthesis by a C-type thermocouple, which was inserted inside a small hole in one side of the graphite die. Temperature, applied current, voltage, mechanical load, and the vertical displacement (δ) of the lower electrode were measured in real time and recorded. The parameter δ can be regarded as the degree of powdered compact densification. In fact, as a consequence of the sample shrinkage, the lower electrode moves up because of the applied mechanical load. However, also thermal expansion of the sample as well as that one of both electrodes, graphite blocks, spacers and plungers, contribute to the variations of this parameter. Therefore, the real degree of consolidation can be gained only by measuring the density of the sample at the end of the process. For the sake of reproducibility, each experiment was repeated at least twice.

After the synthesis process, the sample was first allowed to cool and was then removed from the die. The relative density of the product was determined by geometrical measurements and by the Archimedes method. Phase identification was obtained using a Philips PW 1830 (Almelo, The Netherlands) x-rays diffractometer with Cu K $_{\alpha}$ radiation ($\lambda = 1.5405 \text{ \AA}$) and Ni filter. The microstructure of the end products was examined by scanning electron microscopy (SEM; Hitachi S4000, Tokyo, Japan) and local phase composition was determined by energy dispersive x-ray spectroscopy (EDXS). Phase content in the final product during the kinetic investigation of the process was determined from x-ray diffraction (XRD) patterns by the Rietveld refinement procedure.^{19,20}

An indentation method using a Zwick 3212 (Ulm, Germany) tester machine was used to determine Vickers microhardness and fracture toughness (K_{IC}) of the SPS material. Specifically, the Anstis formula²¹ was used to evaluate the K_{IC} values.

TABLE I. Characteristics of the starting powders used in the present investigation.

Reactant	Source	Particle size	Purity
Tungsten (W)	Aldrich (26,751-1)	12 μm	99.9%
Graphite (C)	Aldrich (28,286-3)	1–2 μm	...
Cobalt (Co)	Aldrich (26,663-9)	<2 μm	99.8

III. RESULTS AND DISCUSSION

A. Kinetic study of the synthesis/densification process

The kinetics of formation of the cemented carbide WC-Co by SPS has been studied by simultaneously applying a constant pulsed electric current (I) and mechanical pressure (P) for different predetermined time intervals, hereafter indicated by ($t_{I \neq 0}$). Specifically, the influence of this parameter on the composition of the obtained SPS products was investigated in the range of $t_{I \neq 0} = 30$ to 240 s, for the case of I and P equal to 800 A and 40 MPa, respectively. The applied current, voltage, temperature, and displacement time profiles recorded during the SPS run corresponding to $t_{I \neq 0} = 240$ s are shown in Fig. 1. Shorter time intervals during which the pulsed electric current is applied, i.e., $t_{I \neq 0} = 30, 60, 90, 120, 150$, and 180 s, are indicated only in Fig. 1, which otherwise would become too confusing.

It may be seen that [compare Fig. 1(a)] the current was augmented from 0 to 800 A in about 20 s and then kept constant to the latter value until the selected $t_{I \neq 0}$ was reached. Correspondingly, when the current was augmented from 0 to 800 A the voltage showed a very rapid

increase until it reached its maximum value, i.e., about 4.8 V. Subsequently, while the current intensity was maintained at the set value of 800 A, the voltage gradually decreased until it dropped to zero when the application of the current was interrupted. The voltage decrease after its maximum value has been reached can be related to the increase of the temperature of the reacting system [compare Fig. 1(b)] encountered during this stage, which is accompanied by a decrease of its electrical resistivity.

The increase of sample temperature with time is a consequence of the heat generation by Joule effect. Although the temperature of the system seems to approach to an asymptotic value, i.e., the thermal equilibrium is reached, this condition is not obtained within the temporal range, i.e., 0–240 s, considered in this study.

The displacement temporal profile shown in Fig. 1(b) reveals that during the first 20 s, i.e., before the current reaches 800 A, the system did not show any noteworthy variation of this parameter. Then δ commenced to slightly rise for about 15–20 s up to 0.08–0.10 mm, but no significant variation is observed in the next 45 s. However, at this point the displacement abruptly increased until it reaches its final value (about 2 mm). It is possible to observe that the rapid sample displacement starts to occur when the temperature is in the range 1000–1100 °C. A further application of the current did not result in any appreciable variation of the displacement, while the observed increase of δ when the application of the electric current was interrupted was a direct consequence of the die/plungers/sample thermal shrinkage which accompanied the cooling of the system.

To monitor the time evolution of reacting system composition during the synthesis of WC-6 wt% Co by SPS, the final samples obtained under the conditions previously examined, i.e., $t_{I \neq 0} = 30, 60, 90, 120, 150$, and 180 s, were analyzed by XRD. The results are reported in Fig. 2. It was found that when the current was applied for 30 and 60 s, only the reactants peaks were detected in the XRD patterns. However, when $t_{I \neq 0}$ was increased to 90 s (compare with Fig. 2), the XRD analysis of the corresponding end-product shows the first evidence of the formation of the final desired product WC along with the appearance of the sub-stoichiometric carbide W_2C . A further increase of $t_{I \neq 0}$ to 120 s resulted in a significant augment of WC content, although W_2C , graphite, and, above all, unreacted tungsten, were still present in the obtained product. However, the latter one strongly decreased when the current was applied for 150 s. In fact, under these experimental conditions, the final product was mainly composed of the desired carbide phase WC with only small traces of the initial reactants, with W_2C also completely absent in the pattern. Finally, as shown in Fig. 2, all the undesired phases disappeared from the XRD pattern, i.e., full conversion of tungsten and graphite to WC was obtained, when $t_{I \neq 0}$ was further

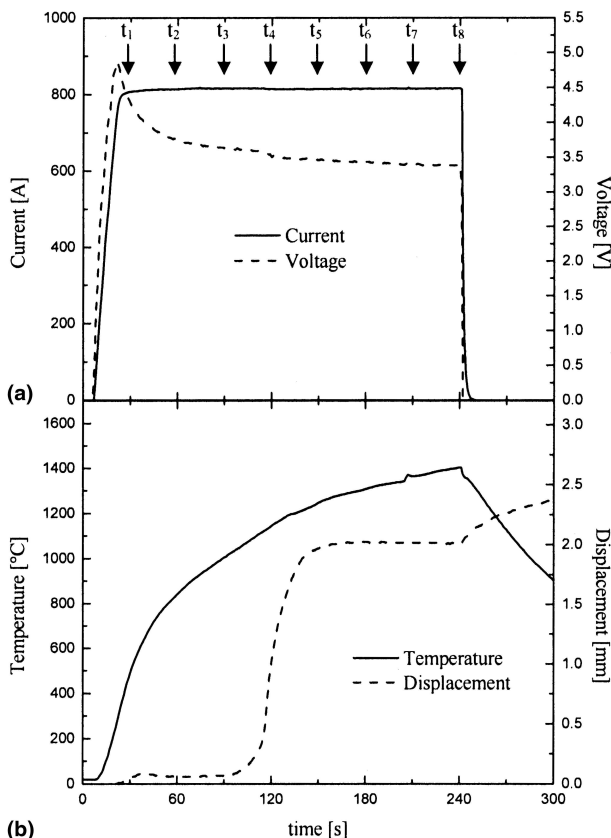


FIG. 1. Temporal profiles of SPS outputs: (a) current intensity and voltage, (b) temperature and sample displacement ($I = 800$ A, $P = 40$ MPa); $t_1 = 30$ s, $t_2 = 60$ s, $t_3 = 90$ s, $t_4 = 120$ s, $t_5 = 150$ s, $t_6 = 180$ s, $t_7 = 210$ s, $t_8 = 240$ s.

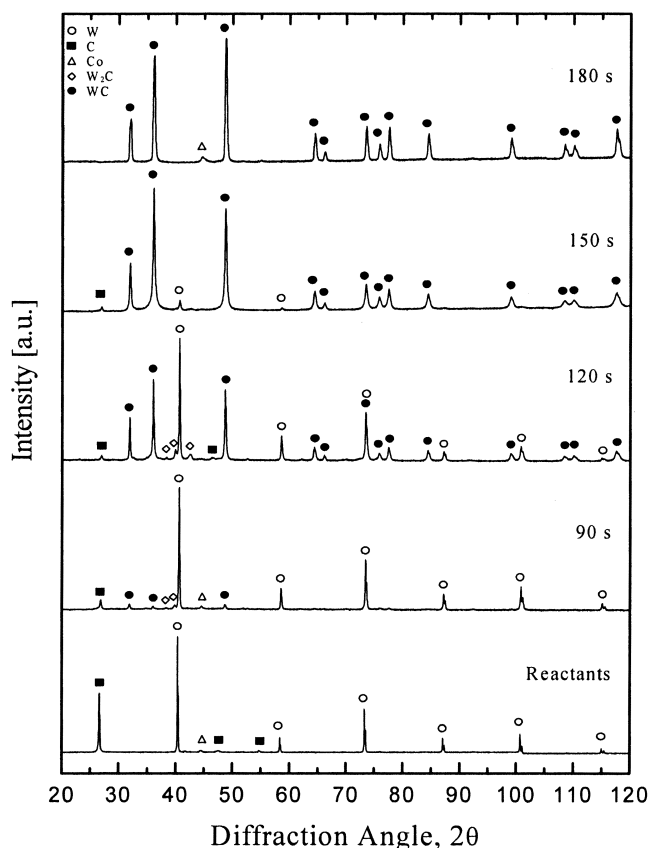


FIG. 2. XRD patterns of SPS products obtained at different values of the time interval during which the pulsed electric current is applied ($I = 800$ A, $P = 40$ MPa).

increased to 180 s. An additional increase of the holding time to 240 s did not produce changes in the final product, i.e., the complete conversion of starting reactants to the desired phase was reached.

It is now possible to correlate the results shown in Fig. 2 with those reported in Figs. 1(a) and 1(b). In fact, by considering the displacement temporal profile [Fig. 1(b)], it is apparent that the rapid increase of δ observed in the time period 90–180 s corresponds to the most significant conversion of W and C to form the final carbide phase WC. As a consequence, the abrupt sample displacement can be associated with the occurrence of the reaction formation of the desired carbide phase.

On the basis of the consideration above, the time at the flex point in the curve showing the displacement temporal profile is defined as the reaction time t_R and the corresponding temperature reached by the system is indicated by T_R . Specifically, under the experimental conditions considered above, i.e., $I = 800$ A, $P = 40$ MPa, t_R and T_R were equal to about 120 s and 1150 °C, respectively.

Quantitative insights on the evolution of the reaction synthesis during SPS can be gained by examining the results shown in Fig. 3, where the relative amount of each

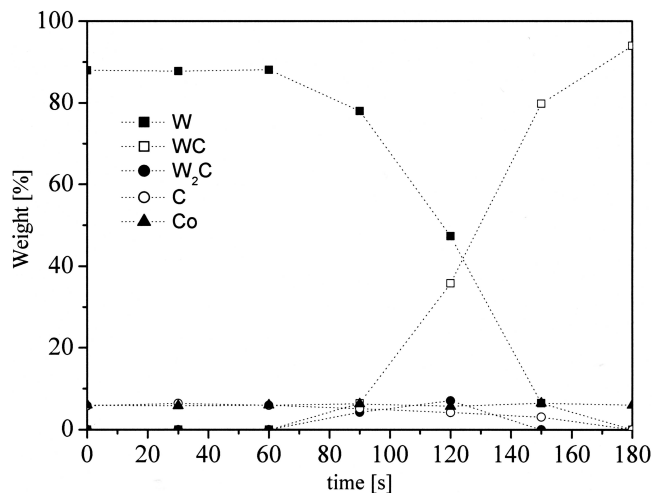
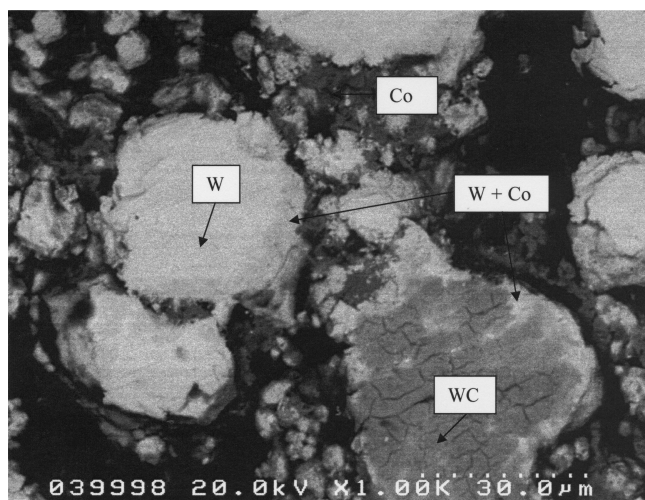


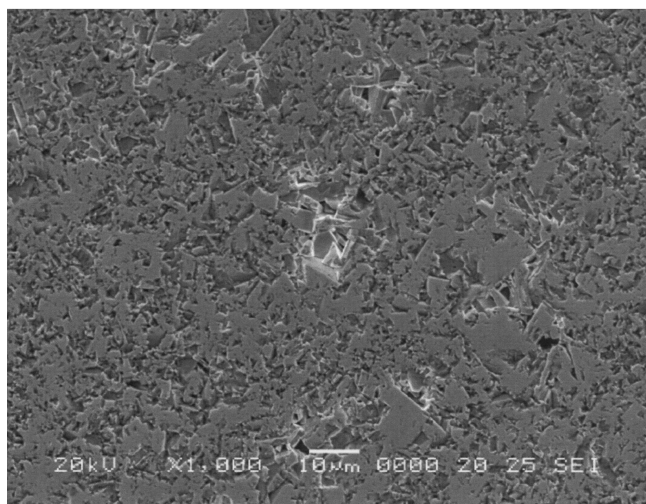
FIG. 3. Relative amount of the different phases detected in the SPS products as a function of the time interval during which the pulsed electric current is applied ($I = 800$ A, $P = 40$ MPa).

phase involved in the process is reported as a function of the time interval during which the pulsed electric current is applied. These results, which are obtained from the XRD analyses as described in the experimental section, still clearly demonstrate that as the conditions where the significant sample displacement is observed, the quantity of W rapidly decreases while WC increases correspondingly. It is interesting to note that the amount of the sub-stoichiometric carbide W_2C in the product first increases then disappears as the holding time is augmented. This can be then considered as an intermediate product in the synthesis reaction to form WC from elemental powders by SPS. This consideration is supported by the results obtained by investigating the carburization process of tungsten powders with carbon.²² In fact, it was found that ditungsten carbide, W_2C , is formed first, and it is only subsequently converted to WC.

Regarding the microstructure characterization of the obtained SPS products, Figs. 4(a) and 4(b) show two SEM micrographs of the samples obtained by applying the pulsed electric current for 120 and 180 s, respectively. In particular, Fig. 4(a) refers to conditions right before the rapid sample displacement occurs [Fig. 1(b)]. From the micrograph shown in Fig. 4(a), it clearly appears that the examined sample is characterized by a very high degree of porosity. In addition, energy dispersive spectroscopy (EDS) analysis revealed that the lighter areas correspond to tungsten while the darker ones are related to cobalt. Graphite cannot be seen due its low molecular weight. It was also inferred that the dark gray regions correspond to the carbide phase at its early stage of formation. In addition, small traces of cobalt were found in the outer areas of the tungsten regions as a consequence of solid diffusion of cobalt into tungsten grains. As a consequence, it clearly appears that the examined sample corresponds to the early stage of the reacting process.



(a)



(b)

FIG. 4. SEM backscattered micrographs of two SPS end-products corresponding to (a) $t_{I \neq 0} = 120$ s and (b) $t_{I \neq 0} = 180$ s ($I = 800$ A, $P = 40$ MPa).

The micrograph shown in Fig. 4(b) is, on the other hand, related to a sample obtained by SPS when interrupting the application of the current after the completion of the rapid displacement ($t_{I \neq 0} = 180$ s), as shown in Fig. 1(b). SEM and EDS results are consistent with XRD analysis (Fig. 2); the sample is characterized by full conversion and relatively high density. The microstructure of the obtained WC/Co composite revealed that it consists of WC grains embedded in the binder phase, even if the latter is not clearly visible due to its low content in the final product.

So far, attention has been mainly focused on the reaction synthesis. However, since the objective of the work is also to obtain a dense material, the consolidation process represents an important issue to be investigated. The evolution of densification phenomena during the synthesis of WC–Co by SPS can be deduced from Fig. 5, in

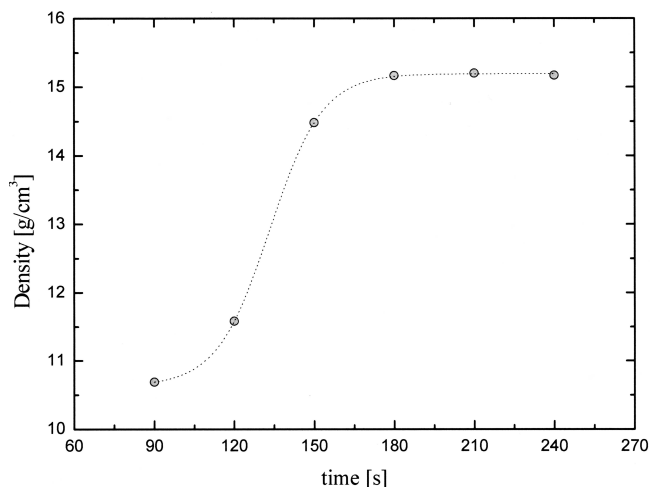


FIG. 5. Densities of end-products obtained by SPS as a function of the time interval during which the pulsed electric current is applied ($I = 800$ A, $P = 40$ MPa).

which the end-products density has been plotted as a function of the time intervals during which the current is applied, $t_{I \neq 0}$. It is seen that the samples obtained when $t_{I \neq 0}$ is relatively short (less than 150 s) show a very high degree of porosity as a consequence of the incomplete sintering process. However, if the time is increased up to 180 s, products characterized by high density, about 15.2 g/cm^3 , i.e., 100% of the theoretical density, are achieved. A further increase of $t_{I \neq 0}$ up to 240 s did not result in significant changes of samples density.

Again, it is important to note that the marked increase in product density takes place when the current is applied for a duration approaching to the previously defined reaction time t_R . This fact allows us to conclude that the synthesis and sintering stages of the WC–6% Co composite by SPS starting from elemental powders take place simultaneously.

In addition, it can be assessed that the synthesis and sintering stages can be considered complete when the displacement–time curve approaches to its asymptotic value, i.e., which required a time interval during which the electric current is applied of 180–200 s [Fig. 1(b)] for the case of the current level, i.e., $I = 800$ A, considered in this study.

B. Effect of the applied current intensity

The effect of the pulsed electric current intensity (I) on the simultaneous synthesis and densification of the composite WC/Co was investigated in the range 600–900 A while the mechanical pressure was maintained constant and equal to 40 MPa for all cases. The application of the electric current was interrupted when the displacement reached its stationary value (plateau). In fact, as discussed in the previous paragraph, under the latter conditions the synthesis and sintering phenomena can be considered complete.

The obtained current, voltage, temperature, and displacement time profiles are shown in Figs. 6(a)–6(d). It is seen that similar profiles from the qualitative point of view are found under the different current levels considered. However [Fig. 6(a)], it is apparent that to obtain the complete conversion and densification of the SPS product lower $t_{I \neq 0}$ values, i.e., the electric power being interrupted earlier, are required as the current level increases.

XRD analyses of the SPS product showed that under the different current levels considered, regardless of the current level applied, a complete conversion of the initial reactants in the final desired carbide phase, WC, was achieved. A close full dense material, i.e., relative density higher than 99%, was also obtained under the entire range of current level investigated.

In addition, voltage increases as the applied current is augmented [Fig. 6(b)] as a consequence of the ohmic behavior of system. The temperature profiles shown in Fig. 6(c) were significantly affected by the level of the applied electric current. Specifically, the heating rate, i.e., the slope of the temperature–time curves, increased as the current level was augmented. This aspect is directly connected to the corresponding relatively higher heat generation by the Joule effect. This result can be also associated with the recorded displacement temporal profiles reported in Fig. 6(d). In fact, it is clearly seen that as the current is augmented, the position of the curves where the rapid sample displacement takes place is anticipated while its slope increases. This means that,

as the heating rate is increased, the onset of the transformation of the elemental reactants to the desired carbide product occurs earlier and the reaction itself becomes faster. These results are summarized in Fig. 7, where the effect of the applied current on the previously defined t_R and T_R values is shown. It is apparent that, while T_R seems not to be appreciably affected by current level, t_R markedly decreases as I increases, being this dependence stronger at lower current levels.

The value of T_R is very close to the minimum temperature of 1050 °C required to obtain full dense WC–10Co by SPS when starting from conventional WC and Co powders.⁹ In fact, the use of temperature lower than the limit above produced only relatively porous product. This behavior was justified by the fact that a complete densification of WC–Co composites was possible only through a mechanism of liquid phase sintering. Consistently, the latter also seems to play a major role in the densification stage in the SPS process investigated in this work.

Regarding this aspect, during sintering of WC–Co, considerable shrinkage was observed to occur at temperature slightly higher than 1200 °C, i.e., not only before the melting point of cobalt ($T = 1495$ °C) is reached, but also before the eutectic liquid WC–Co is formed ($T = 1350$ °C).^{3,23} Although the T_R value is lower than 1200 °C, it is worth noting that, as reported in the Sec. II, temperature measurements were performed in the graphite die using a thermocouple inserted inside a small hole. Therefore, it is likely that the temperature in

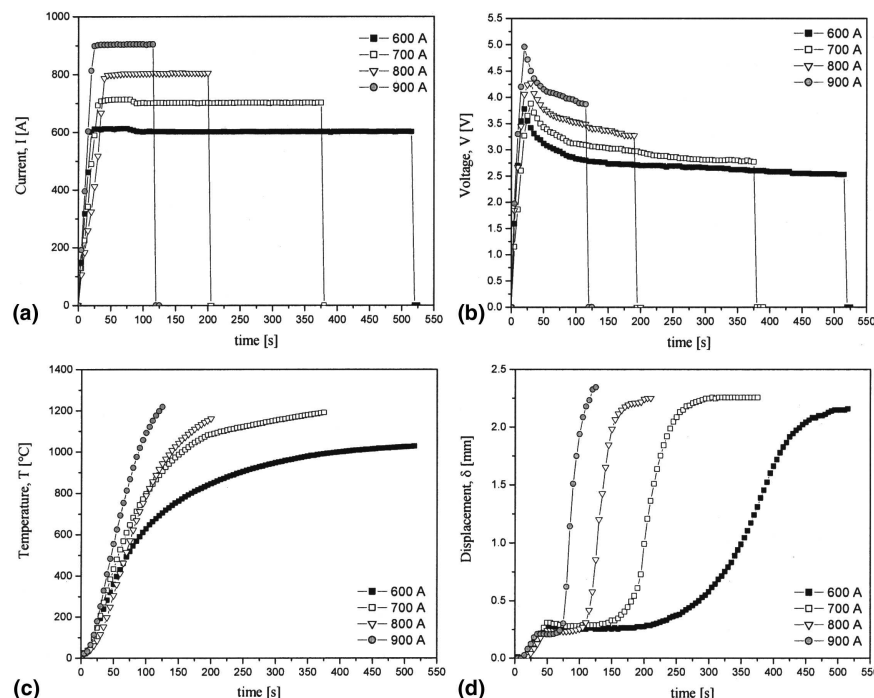


FIG. 6. Temporal profiles of SPS outputs obtained at different levels (600–900 A) of the applied current: (a) current intensity, (b) voltage, (c) temperature, and (d) sample displacement ($P = 40$ MPa).

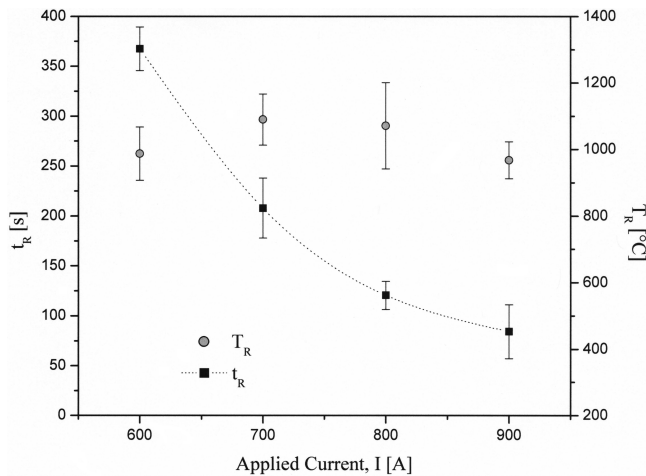


FIG. 7. Dependence of t_R and T_R on the applied current level.

the reacting sample is higher and can locally reach the value above.

Vickers microhardness measurements were performed on polished SPS composites samples using a 294.3 N (30 kg) indentation load and 15 s dwell time. The corresponding hardness value, as a result of ten measurements, was found to be equal to 14.97 ± 0.35 GPa. In particular, this result refers to products obtained when $I = 800$ A and $t_{I \neq 0} = 240$ s. The estimation of fracture toughness of the SPS material was determined using the Anstis formula²¹ as follows

$$K_{IC} = 0.016 \left(\frac{E}{H} \right)^{0.5} \frac{P}{L^{1.5}},$$

where K_{IC} is the fracture toughness of the material, E is the Young's modulus, H is the hardness, P is the applied load, and L is the length of the crack measured from the center of the indentation. The average of ten measurements provides a calculated fracture toughness equal to $12.5 \text{ MPa m}^{0.5}$ and an uncertainty of $\pm 1.0 \text{ MPa m}^{0.5}$.

The obtained values are very similar to, sometimes better than, the best results reported in the literature for WC–Co dense products based on the same nominal composition, particularly when considering fracture toughness characteristics.^{3,13} Specifically, while the hardness of the synthesized SPS material is a little lower than the value of 15.5 GPa reported by Upadhyaya³ for commercial dense WC–6 wt%Co products, the calculated fracture toughness observed in this work is greater than the corresponding reported value of $9.6 \text{ MPa m}^{0.5}$.³ This characteristic is still in evidence when the comparison is extended to the WC–Co composite materials with the same or very close nominal composition, i.e., the cobalt content is in the range 5.9–6.0 wt%, obtained from alternative conventional and innovative techniques, for instance one-step FAPACS.¹³ First, it is reported that the

WC–5.9 wt% Co products obtained using the FAPACS method, which is similar to the technique considered in this work, appear to be superior in terms of microhardness (18.6 GPa) to those ones produced by conventional techniques.¹³ This is also true when the comparison includes the SPS products obtained in this work. However, regarding fracture toughness, a much higher value ($12.5 \text{ MPa m}^{0.5}$) was obtained in our case, since it was found to be $8.6 \text{ MPa m}^{0.5}$ for the case of WC–5.9 wt% Co samples produced by FAPACS, and values up to $10.0 \text{ MPa m}^{0.5}$ were reported for WC–6 wt% Co using conventional techniques.¹³

In addition, Park et al.¹³ showed that an augment of the Co content in the composite up to 12.5 wt% Co produced only a slight increase of the fracture toughness up to $9.4 \text{ MPa m}^{0.5}$, while the corresponding hardness decreased more significantly to 16.4 GPa.

The observed difference of structural characteristics of products obtained using FAPACS or SPS may be explained on the basis of different products density, i.e., higher than 99% theoretical value for SPS product and in the range 97–98% for the similar one (5 vol% Co content equivalent to 5.9 wt% Co), prepared using FAPACS.¹³ This result is related to different operating conditions encountered during the two synthesis/densification processes. Firstly, a direct current is used in the FAPACS apparatus while the SPS technique is based on the use of a pulsed current, which could play an important role in the synthesis/densification process.^{12,15} In addition, a current intensity of 3000 A (which corresponds to a current density, calculated by considering the die or the plunger cross sections, of about 2400 or 9550 kA/m², respectively) and a mechanical pressure of 60 MPa, are adopted during the FAPACS process. On the other hand, lower current, i.e., 800 A (corresponding to a current density, calculated by considering the die or the plunger cross sections, of about 1130 or 4530 kA/m², respectively), as well as smaller mechanical pressure (40 MPa) levels are used during the SPS procedure. Moreover, as described in the experimental section, the use of graphite felt in the SPS process to cover the graphite die with the aim of minimizing heat losses by thermal radiation, can also affect the temperature distribution inside the sample and consequently the final product microstructure.

IV. CONCLUDING REMARKS

The synthesis and consolidation of the WC–6Co cemented carbide starting from elemental W, C, and Co, powders was obtained in a single-step process by taking advantage of the SPS technology.

The application of an electric pulsed current of 800 A and a mechanical pressure of 40 MPa for about 200 s, allows for the obtainment of a pure dense product (relative density higher than 99%). The latter one displayed a

Vickers microhardness and fracture toughness values of 14.97 ± 0.35 GPa, and 12.5 ± 1.0 MPa m^{0.5}, respectively.

A kinetic study of the synthesis process has been first performed. This investigation was based on the monitoring of product composition and density as the time interval during which the pulsed electric current is applied was gradually increased. The conditions for obtaining the complete conversion of the starting reactants to the desired full dense material have been identified. In particular, the synthesis and sintering stages, which are observed to occur simultaneously, can be considered completed when the displacement–time curve approaches an asymptotic value. In addition, by examining product compositional changes in parallel with sample displacement, it was found that the observed relatively rapid sample shrinkage, corresponded to a significant decrease of W and WC increase. However, the first carbide formed appeared to be the intermediate phase W₂C, which, as the SPS holding time was augmented, was gradually converted to WC.

The dependence of process dynamics on the electric current level was then examined systematically. As the applied current intensity was augmented, the time where the maximum densification rate was observed to occur, considerably decreased, being this effect more significant when operating at low current levels. In addition, the corresponding temperature did not change appreciably as the current was varied. This fact was associated to a liquid phase sintering mechanism which is governing the densification process.

ACKNOWLEDGMENTS

The financial support of MIUR-PROMEA (D.M. n.1015, 04/10/2001), MIUR-PRIN (2002), PRISMA-INSTM (2003), Italy, is gratefully acknowledged. The activity performed by Mrs. Sara Todde is also gratefully acknowledged. In addition, the authors would like to thank Dr. Leonardo Esposito, Centro Ceramico di Bologna, Italy, for structural characterization of SPS samples.

REFERENCES

1. G.S. Upadhyaya: *Cemented Tungsten Carbides: Production, Properties, and Testing* (Noyes Publications, Norwich, NY, 1998).
2. Z.G. Fang, G. Lockwood, and A. Griffo: A dual composite of WC-Co. *Metall. Mater. Trans. A* **30**(12), 3231 (1999).
3. G.S. Upadhyaya: Materials science of cemented carbides—An overview. *Mater. Des.* **22**, 483 (2001).
4. L. Fu, L.H. Cao, and Y.S. Fan: Two-step synthesis of nanostructured tungsten-carbide-cobalt powders. *Scripta Mater.* **44**, 1061 (2001).
5. G-Q. Shao, X-L. Duan, J-R. Xie, X-H. Yu, W-F. Zhang, and R-Z. Yuan: Sintering of nanocrystalline WC–Co composite powder. *Rev. Adv. Mater. Sci.* **5**, 281 (2003).
6. M.A. Xueming and J.I. Gang: Nanostructured WC–Co alloy prepared by mechanical alloying. *J. Alloys Compd.* **245**, L30 (1996).
7. M.S. El-Eskandarany, M. Omori, M. Ishikuro, T.J. Konno, K. Takada, K. Sumiyama, T. Hirai, and K. Suzuki: Synthesis of full-density nanocrystalline tungsten carbide by reduction of tungstic oxide at room temperature. *Metall. Mater. Trans. A* **27A**, 4210 (1996).
8. M.S. El-Eskandarany, A.A. Mahday, H.A. Ahmed, and A.H. Amer: Synthesis and characterization of ball-milled nanocrystalline WC and nanocomposite WC-Co powders and subsequent consolidation. *J. Alloys Compd.* **312**, 315 (2000).
9. S.I. Cha, S.H. Hong, and B.K. Kim: Spark plasma sintering behavior of nanocrystalline WC-10Co cemented carbide powders. *Mater. Sci. Eng. A* **A315**, 31 (2003).
10. J. Zhang, J.H. Lee, D.Y. Maeng, and C.W. Won: Synthesis of tungsten monocarbide by self-propagating high-temperature synthesis in the presence of an activative additive. *J. Mater. Sci.* **36**, 3233 (2001).
11. L.H. Zhu, Q.W. Huang, and H.F. Zhao: Preparation of nanocrystalline WC–10Co–0.8VC by spark plasma sintering. *J. Mater. Sci. Lett.* **22**, 1631 (2003).
12. M. Tokita: Large-size functionally graded materials fabricated by spark plasma sintering (SPS). *Method. Mater. Sci. Forum* **423–425**, 39 (2003).
13. C-D. Park, H-C. Kim, I-J. Shon, and Z.A. Munir: One-step synthesis of dense tungsten carbide-cobalt hard materials. *J. Am. Ceram. Soc.* **85**(11), 2670 (2002).
14. H-C. Kim, D-Y. Oh, and I-J. Shon: Synthesis of WC and dense WC-x vol.%Co hard materials by high-frequency induction heated combustion method. *Int. J. Refractory Metals Hard Mater.* **22**, 41 (2004).
15. M. Omori: Sintering, consolidation, reaction and crystal growth by spark plasma sintering (SPS). *Mater. Sci. Eng. A* **287**, 183 (2000).
16. M. Kawahara, H-T. Kim, and M. Tokita: Fabrication of nanomaterials by spark plasma sintering (SPS) method, in *Proc. 2000 Metallurgy World Congress* (Japan Society of Powder and Powder Metallurgy, Kyoto, Japan, 2000), p. 741.
17. R. Orrù, J. Woolman, G. Cao, and Z.A. Munir: The synthesis of dense nanometric MoSi₂ through mechanical and field activation. *J. Mater. Res.* **16**, 1439 (2001).
18. Z.J. Shen, M. Johnsson, Z. Zhao, and M. Nygren: Spark plasma sintering of alumina. *J. Am. Ceram. Soc.* **85**(8), 1921 (2002).
19. A.M. Rietveld: A profile refinement method for nuclear and magnetic structures. *J. Appl. Crystallogr.* **2**, 65 (1969).
20. L. Lutterotti, R. Ceccato, R. Dal Maschio, and E. Pagani: Quantitative analysis of silicate glass in ceramic materials by the Rietveld method. *Mater. Sci. Forum* **278–281**, 87 (1998).
21. G.R. Anstis, P. Chantikul, B.R. Lawn, and D.B. Marshall: A critical evaluation of indentation techniques for measuring fracture toughness: I. Direct crack measurements. *J. Am. Ceram. Soc.* **64**(9), 533 (1981).
22. L.V. McCarty, R. Donelson, and R.F. Hehemann: A diffusion model for tungsten powder carburization. *Metall. Mater. Trans. A* **18A**, 969 (1987).
23. R.M. German: *Liquid Phase Sintering* (Plenum Press, New York, 1985).